The 2013 World Congress on
Advances in Structural Engineering and Mechanics (ASEM13)
Jeju, Korea, September 8-12, 2013

Finite element analysis of pedestrian-floor dynamic interaction including human participation

*Jingwei Qin[1)], Qingshan Yang[2)] and Siu Seong Law[3)]

[1), 2)] *School Civil Engineering, Beijing Jiaotong University, Beijing, China*
[3)] *Department of Civil and Environmental Engineering, The Hong Kong Polytechnic University, Hong Kong, China*
[1)] qinjingwei74@gmail.com

ABSTRACT

The pedestrian-floor dynamic interaction problem based on bipedal walking model and damped compliant legs is presented in this work. The classical finite element method combined with a moving finite element to represent the motion of pedestrian is used to perform the dynamic analysis of floor. A control force with consideration of deflection of the structure is applied by the pedestrian to compensate for the energy dissipated with system damping in walking and to regulate the walking performance of the pedestrian. Numerical simulations are performed to highlight the features of the proposed pedestrian-floor dynamic interaction model. Simulation results show that the dynamic interaction will increase with a larger vibration level of structure. Results indicate that the simple bipedal walking model could well describe the human-structure dynamic interaction.

1. INTRODUCTION

Vibration serviceability has become a governing design criterion for modern light and slender structures dynamically excited by human walking, such as the long-span office floors and waiting room. Human–structure interaction (HSI) is a complex, interdisciplinary and less researched topic in the design of these structures. For a slender and long-span floor structure, excessive vibration may easily occur due to human walking creating a vibration serviceability problem.

Since footbridges are much more responsive in the lateral direction, the bridge vibration and the force model have been research extensively. Amongst the many models of lateral pedestrians loading, a biomechanically model of the pedestrian response to the lateral bridge motion was presented and explored (Macdonald 2008; Morbiato, *et al* 2011; Bocian *et al* 2012). These simple models captured the key features of the lateral balance of a pedestrian and the resulting forces on the structure. In contrast to the footbridge, the floors are much more responsive in the vertical direction. Inspired by the above researches, a simple model was developed to describe the pedestrian-floor interaction based on a bipedal walking model (Geyer et al 2006; Whittington and Thelen 2009; Kim and Park 2011) with input from biomechanical engineering.

[1)] PhD student
[2),3)] Professor

Vibration of a structure under moving external effects has been well studied by many researchers. Some of them introduced a moving finite element in the dynamic analysis of structures (Yang et al 1999; Yang and Wu 2001; Wu 2008; İsmail 2011).
This paper presents a "moving finite element" in the dynamic analysis of structure under the pedestrian motion modeled with a bipedal walking model. The classical finite element method is combined with the moving finite element to represent the pedestrian motion with all effects. The equations of motion of the human-structure system will be derived, in which a control force in the feedback manner is provided by the pedestrian to compensate for energy dissipation in the system damping in walking and to regulate the walking performance of the pedestrian. Numerical simulations are performed to highlight the features of the proposed model. Finally, an experiment with a pedestrian walking on a simply supported floor slab was conducted to validate the performance of the proposed interaction model.

2. FORMULATION

2.1 Bipedal walking model

Fig. 1 shows that the human body modeled as a lumped mass m_h at the center of mass (CoM) and it describes the legs as two massless, linear springs of equal rest length l_0 and stiffness k_{leg} with time-variant damper neglecting the roller feet. A passive spring provides a compliant mechanism to absorb collision impacts and to generate push-off impulses, whereas the damper restrained excessive motion of the CoM (Kim and Park, 2011). Both springs and damper act independently and influence the model dynamics only during stance when the spring and damper force oppose the gravitational force of the human body.
A complete step, which is defined as the interval between ‘heel strike’ of two feet, is divided into two phases: single support and double support. For example, the double support phase begins with ‘touch down’ (TD) of the leading leg and ends with ‘touch off’ (TO) of the trailing leg as shown in Fig. 1, where the single support phase begins. Then, the trailing leg is repositioned ahead of the body’s CoM at a given angle of attack and becomes the leading leg for the next step. When the trailing leg hits the ground, the single support phase is finished.

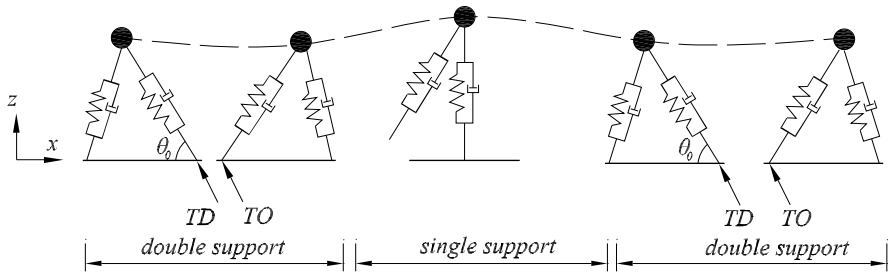

Fig. 1 Schematic of the biomechanical walking model (θ_0 is angle of attack)

2.2 System matrices of the moving finite element

Fig. 2 shows the finite element mesh of a rectangular plate under a pedestrian and the *i*th and *j*th plate elements on which the pedestrian applies its load at time 't'. The plate has m×n elements and (m+1)×(n+1) nodes with three degrees-of-freedom at each node. The time-dependent global position of the pedestrian on the plate element is $\bar{x}_c(t)$, while the local position on the length of the element is $x_c(t)$. In this study, the subscripts *i* and *j* are used to denote quantities associated with the leading and trailing leg in double support phase, respectively. A four-node plate element based on the Mindlin theory including the effect of transverse shear deformation is adopted in this study. The pedestrian is assumed to walk forward along a straight line.

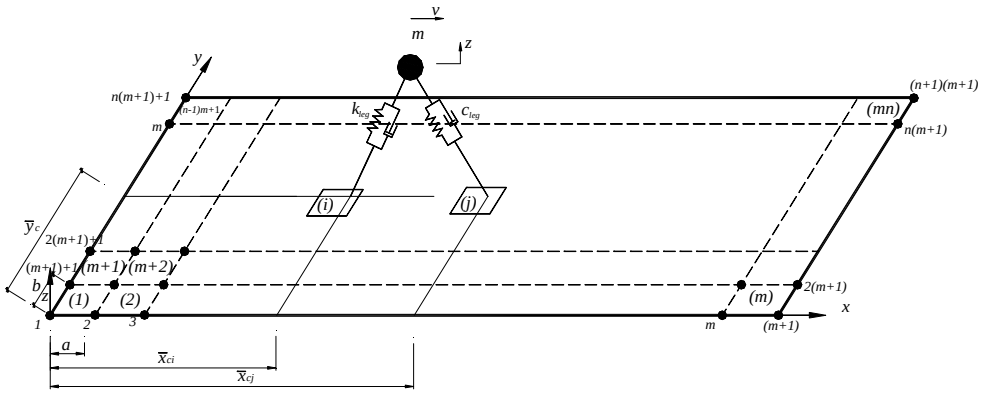

Fig. 2 A rectangular plate composed of (m+1)×(n+1) nodes

The process described below is based on the mechanical properties of the system in the double support phase. In fact, the process for the single support phase is the same as the double support phase. The equations of motion can finally be expressed in the same form for both phases.

Fig. 3 shows the free body diagrams for the components of the HSI system. The pedestrian is acted upon by the elastic forces $F_{s,t}$, $F_{s,l}$, damping forces, $F_{d,t}$, $F_{d,l}$, inertial force F_I and the gravitational force G, and the supporting floor is acted upon by the the elastic forces $F_{s,t}$, $F_{s,l}$ and the damping forces, $F_{d,t}$, $F_{d,l}$. The subscripts 'l' and 't' indicate the leading and trailing legs, respectively. The elastic forces between the components can be given as:

$$F_{s,l} = k_{leg}(L_l(t) - L_0) \tag{1-a}$$

$$F_{s,t} = k_{leg}(L_t(t) - L_0) \tag{1-b}$$

Where $L_l(t)$, $L_t(t)$, L_0 are the time-varying lengths of the leading and trailing legs and the rest length of leg, respectively.

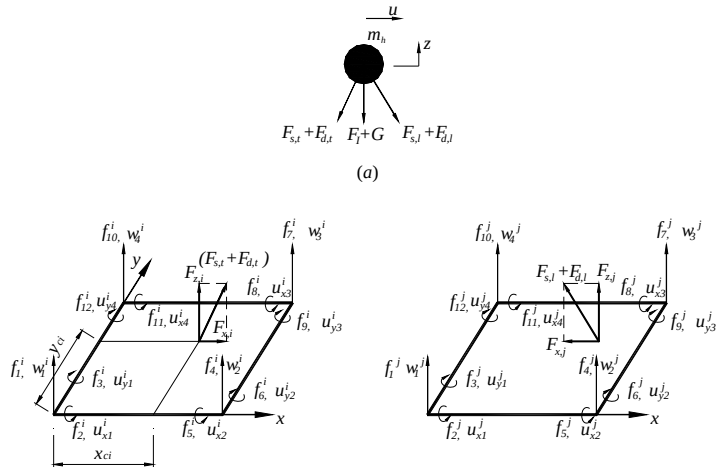

(*a*)

(*b*) the *i*th plate element (*c*) the *j*th plate element

Fig. 3 The equivalent nodal forces and moments corresponding to the contact force applied on the ith and jth plate element

The damping forces based on the time variant damping assumption (Qin *et al* 2013) can be given as:

$$F_{d,l} = \alpha(t) c_{leg} v_l \tag{2-a}$$

$$F_{d,t} = (1-\alpha(t)) c_{leg} v_t \tag{2-b}$$

$$\alpha(t) = \frac{L_t(t) - L_t(0)}{l_0 - L_t(0)} \tag{2-c}$$

Where $\alpha(t)$ is the coefficient of damping; v_l, v_t are the damping and axial velocity of the leading and trailing legs, respectively; L_t (0) is the length of the trailing leg at the start of the double support phase.

The time-varying lengths of two legs are given by

$$L_l(t) = \sqrt{(\sum_{k=1}^{N} d_k - u)^2 + (z - \omega\big|_N)^2} \tag{3-a}$$

$$L_t(t) = \sqrt{(u - \sum_{k=1}^{N-1} d_k)^2 + (z - \omega\big|_{N-1})^2} \tag{3-b}$$

Where *z* and *u* denote the vertical and horizontal displacement of CoM. d_k, $\omega\big|_N$ and $\omega\big|_{N-1}$ are the *k*th step length, the displacement of plate corresponding to the leading and trailing legs in the *N*th step cycle under consideration, respectively.

The axial velocity can be given by the derivative of the length of legs as

$$v_l = (\dot{z} - \dot{\omega}\big|_N)\sin\theta_l - \dot{u}\cos\theta_l \tag{4-a}$$

$$v_t = (\dot{z} - \dot{\omega}\big|_{N-1})\sin\theta_t + \dot{u}\cos\theta_t \tag{4-b}$$

Where θ_l, θ_t are the angle of attack of the leading and trailing legs respectively. Substituting Eqs. (3) and (4) into Eqs. (1) and (2) gives

$$F_{s,l} = k_{leg}\left(L_l(t) - l_0\right) = k_{leg}\left(\sqrt{(\sum_{i=1}^{N} d_i - u)^2 + (z - \omega\big|_N)^2} - l_0\right) \tag{5-a}$$

$$F_{s,t} = k_{leg}\left(L_t(t) - l_0\right) = k_{leg}\left(\sqrt{(u - \sum_{i=1}^{N-1} d_i)^2 + (z - \omega\big|_{N-1})^2} - l_0\right) \tag{5-b}$$

$$F_{d,l} = \alpha(t)c_{leg}\left((\dot{z} - \dot{\omega}\big|_N)\sin\theta_l - \dot{u}\cos\theta_l\right) \tag{5-c}$$

$$F_{d,t} = \left(1-\alpha(t)\right)c_{leg}\left((\dot{z} - \dot{\omega}\big|_{N-1})\sin\theta_t + \dot{u}\cos\theta_t\right) \tag{5-d}$$

The contact force *F* consists of the transverse force component F_z and the longitudinal force component F_x in $\mathbf{F}_i = \left\{F_{x,i} \quad F_{z,i}\right\}^T$, $\mathbf{F}_j = \left\{-F_{x,j} \quad F_{z,j}\right\}^T$. Then the components can be written as

$$F_{z,i} = (F_{s,t} + F_{d,t})\sin\theta_t \tag{6-a}$$

$$F_{x,i} = (F_{s,t} + F_{d,t})\cos\theta_t \tag{6-b}$$

$$F_{z,j} = (F_{s,l} + F_{d,l})\sin\theta_l \tag{6-c}$$

$$F_{x,j} = (F_{s,l} + F_{d,l})\cos\theta_l \tag{6-d}$$

Substituting Eq. (5) into Eq. (6) gives

$$\begin{aligned} F_{z,i} = {} & k_{leg}\left(1 - l_0 / L_t(t)\right)\left(z - \omega\big|_{N-1}\right) + \left(1-\alpha(t)\right)c_{leg}\left(\dot{z} - \dot{\omega}\big|_{N-1}\right)\sin^2\theta_t \\ & + \left(1-\alpha(t)\right)c_{leg}\dot{u}\sin\theta_t\cos\theta_t \end{aligned} \tag{7-a}$$

$$\begin{aligned} F_{x,i} = {} & k_{leg}\left(1 - l_0 / L_t(t)\right)\left(u - \sum_{i=1}^{N-1} d_i\right) + \left(1-\alpha(t)\right)c_{leg}\left(\dot{z} - \dot{\omega}\big|_{N-1}\right)\sin\theta_t\cos\theta_t \\ & + \left(1-\alpha(t)\right)c_{leg}\dot{u}\cos^2\theta_t \end{aligned} \tag{7-b}$$

$$\begin{aligned} F_{z,j} = {} & k_{leg}\left(1 - l_0 / L_l(t)\right)\left(z - \omega\big|_N\right) + \alpha(t)c_{leg}\left(\dot{z} - \dot{\omega}\big|_N\right)\sin^2\theta_l \\ & - \alpha(t)c_{leg}\dot{u}\sin\theta_l\cos\theta_l \end{aligned} \tag{7-c}$$

$$\begin{aligned} F_{x,j} = {} & k_{leg}\left(1 - l_0 / L_l(t)\right)\left(\sum_{i=1}^{N} d_i - u\right) + \alpha(t)c_{leg}\left(\dot{z} - \dot{\omega}\big|_N\right)\sin\theta_l\cos\theta_l \\ & - \alpha(t)c_{leg}\dot{u}\cos^2\theta_l \end{aligned} \tag{7-d}$$

Obviously, the contact forces acting on the *i*th and *j*th elements are affected not only by the dynamic responses of structure at the contact point, but also by that of the human body, i.e. coupling exists between the pedestrian and the structure.
The nodal forces of the *i*th and *j*th plate elements are given by

$$\mathbf{f}_i = \left\{ f_1^i \quad f_2^i \quad f_3^i \quad \cdots \quad f_{12}^i \right\}^T \tag{8-a}$$

$$\mathbf{f}_j = \left\{ f_1^j \quad f_2^j \quad f_3^j \quad \cdots \quad f_{12}^j \right\}^T \tag{8-b}$$

Where

$$f_3^i = F_{z,i} H_1^i(\xi,\eta), \quad f_6^i = F_{z,i} H_2^i(\xi,\eta), \quad f_9^i = F_{z,i} H_3^i(\xi,\eta),$$
$$f_{12}^i = F_{z,i} H_4^i(\xi,\eta),$$
$$f_1^i = f_2^i = f_4^i = f_5^i = f_7^i = f_8^i = f_{10}^i = f_{11}^i = 0 \tag{9-a}$$
$$f_3^j = F_{z,j} H_1^j(\xi,\eta), \; f_6^j = F_{z,j} H_2^j(\xi,\eta), \; f_9^j = F_{z,j} H_3^j(\xi,\eta),$$
$$f_{12}^j = F_{z,j} H_4^j(\xi,\eta)$$
$$f_1^j = f_2^j = f_4^j = f_5^j = f_7^j = f_8^j = f_{10}^j = f_{11}^j = 0 \tag{9-b}$$

Where $H_k^i(\xi,\eta)$ and $H_k^j(\xi,\eta)$ (*k*=1~4) are shape functions of the *i*th and *j*th plate element. The nodal forces depend on the location of the contact point of walking load relative to the plate. The shape functions of the *i*th plate element can be given by (Kwon,1996):

$$\begin{aligned} H_1^i(\xi,\eta) &= \frac{1}{4}(1-\xi)(1-\eta) \\ H_2^i(\xi,\eta) &= \frac{1}{4}(1+\xi)(1-\eta) \\ H_3^i(\xi,\eta) &= \frac{1}{4}(1+\xi)(1+\eta) \\ H_4^i(\xi,\eta) &= \frac{1}{4}(1-\xi)(1+\eta) \end{aligned} \tag{10}$$

with the natural coordinate (ξ, η):

$$\xi = \frac{x_{ci}(t) - x_0^i}{a}, \quad \eta = \frac{y_{ci}(t) - y_0^i}{b} \tag{11}$$

where a and b are half of the length and width of the ith plate element; $x_{ci}(t)$ and $y_{ci}(t)$ are the local coordinates in the *i*th plate element; x_0^i and y_0^i are the center of the *i*th plate element at time 't', as shown in Fig. 3.

The nodal displacement vectors of the plate element are expressed as follows:

$$\mathbf{u}_i^e = \left\{\theta_{x1}^i \quad \theta_{y1}^i \quad \omega_1^i \quad \theta_{x2}^i \quad \theta_{y2}^i \quad \omega_2^i \quad \theta_{x3}^i \quad \theta_{y3}^i \quad \omega_3^i \quad \theta_{x4}^i \quad \theta_{y4}^i \quad \omega_4^i\right\}^T \tag{12-a}$$

$$\mathbf{u}_j^e = \left\{\theta_{x1}^j \quad \theta_{y1}^j \quad \omega_1^j \quad \theta_{x2}^j \quad \theta_{y2}^j \quad \omega_2^j \quad \theta_{x3}^j \quad \theta_{y3}^j \quad \omega_3^j \quad \theta_{x4}^j \quad \theta_{y4}^j \quad \omega_4^j\right\}^T \tag{12-b}$$

Based on the definition of the shape functions, the vertical displacements of the plate element at the foot point can be obtained from

$$\omega\big|_{N-1} = \sum_{k=1}^{4} H_k^i(\xi,\eta)\omega_k^i \tag{13-a}$$

$$\omega\big|_{N} = \sum_{k=1}^{4} H_k^j(\xi,\eta)\omega_k^j \tag{13-b}$$

where ω_k^i (*k*=1~4) and ω_k^j (k=1~4) are the nodal transverse displacement of the *i*th and *j*th element.

The velocities $\dot{\omega}\big|_{N-1}$ and $\dot{\omega}\big|_{N}$ are computed as the differential of the function $\omega\big|_{N-1}$ and $\omega\big|_{N}$ respectively with respect to time '*t*':

$$\dot{\omega}\big|_{N-1} = \frac{\mathrm{d}(\omega\big|_{N-1})}{\mathrm{d}\,t} = \sum_{k=1}^{4} H_k^i(\xi,\eta)\dot{\omega}_k^i \tag{14-a}$$

$$\dot{\omega}\big|_{N} = \frac{\mathrm{d}(\omega\big|_{N})}{\mathrm{d}\,t} = \sum_{k=1}^{4} H_k^j(\xi,\eta)\dot{\omega}_k^j \tag{14-b}$$

Substituting Eqs. (13), (14) and (7) into Eq. (9) gives the equations of the moving finite element

$$\mathbf{f}_i = \left\{f_1^i \quad f_2^i \quad f_3^i \quad \ldots \quad f_{12}^i\right\}^T = \mathbf{C}_i\dot{\mathbf{u}}_i^e + \mathbf{K}_i\mathbf{u}_i^e + \mathbf{C}_{pi}\dot{\mathbf{u}}_h + \mathbf{K}_{pi}\mathbf{u}_h \tag{15-a}$$

$$\mathbf{f}_j = \left\{f_1^j \quad f_2^j \quad f_3^j \quad \ldots \quad f_{12}^j\right\}^T = \mathbf{C}_j\dot{\mathbf{u}}_j^e + \mathbf{K}_j\mathbf{u}_j^e + \mathbf{C}_{pj}\dot{\mathbf{u}}_h + \mathbf{K}_{pj}\mathbf{u}_h \tag{15-b}$$

where

$$\mathbf{C}_i = -(1-\alpha(t))c_3\begin{bmatrix}
0 & 0 & 0 & 0 & 0 & 0 & 0 & 0 & 0 & 0 & 0 & 0 \\
0 & 0 & 0 & 0 & 0 & 0 & 0 & 0 & 0 & 0 & 0 & 0 \\
0 & 0 & H_1^iH_1^i & 0 & 0 & H_1^iH_2^i & 0 & 0 & H_1^iH_3^i & 0 & 0 & H_1^iH_4^i \\
0 & 0 & 0 & 0 & 0 & 0 & 0 & 0 & 0 & 0 & 0 & 0 \\
0 & 0 & 0 & 0 & 0 & 0 & 0 & 0 & 0 & 0 & 0 & 0 \\
0 & 0 & H_2^iH_1^i & 0 & 0 & H_2^iH_2^i & 0 & 0 & H_2^iH_3^i & 0 & 0 & H_2^iH_4^i \\
\ldots & \ldots & \ldots & \ldots & \ldots & \ldots & \ldots & \ldots & \ldots & \ldots & \ldots & \ldots \\
0 & 0 & 0 & 0 & 0 & 0 & 0 & 0 & 0 & 0 & 0 & 0 \\
0 & 0 & 0 & 0 & 0 & 0 & 0 & 0 & 0 & 0 & 0 & 0 \\
0 & 0 & H_4^iH_1^i & 0 & 0 & H_4^iH_2^i & 0 & 0 & H_4^iH_3^i & 0 & 0 & H_4^iH_4^i
\end{bmatrix}$$

$$\mathbf{K}_i = -k_3 \begin{bmatrix} 0 & 0 & 0 & 0 & 0 & 0 & 0 & 0 & 0 & 0 & 0 & 0 \\ 0 & 0 & 0 & 0 & 0 & 0 & 0 & 0 & 0 & 0 & 0 & 0 \\ 0 & 0 & H_1^i H_1^i & 0 & 0 & H_1^i H_2^i & 0 & 0 & H_1^i H_3^i & 0 & 0 & H_1^i H_4^i \\ 0 & 0 & 0 & 0 & 0 & 0 & 0 & 0 & 0 & 0 & 0 & 0 \\ 0 & 0 & 0 & 0 & 0 & 0 & 0 & 0 & 0 & 0 & 0 & 0 \\ 0 & 0 & H_2^i H_1^i & 0 & 0 & H_2^i H_2^i & 0 & 0 & H_2^i H_3^i & 0 & 0 & H_2^i H_4^i \\ \dots & \dots & \dots & \dots & \dots & \dots & \dots & \dots & \dots & \dots & \dots & \dots \\ 0 & 0 & 0 & 0 & 0 & 0 & 0 & 0 & 0 & 0 & 0 & 0 \\ 0 & 0 & 0 & 0 & 0 & 0 & 0 & 0 & 0 & 0 & 0 & 0 \\ 0 & 0 & H_4^i H_1^i & 0 & 0 & H_4^i H_2^i & 0 & 0 & H_4^i H_3^i & 0 & 0 & H_4^i H_4^i \end{bmatrix}$$

$$\mathbf{C}_{pi} = (1 - a(t)) \begin{bmatrix} 0 & 0 \\ 0 & 0 \\ c_3 H_1^i & c_4 H_1^i \\ 0 & 0 \\ 0 & 0 \\ c_3 H_2^i & c_4 H_2^i \\ \dots & \dots \\ 0 & 0 \\ 0 & 0 \\ c_3 H_4^i & c_4 H_4^i \end{bmatrix} \qquad \mathbf{K}_{pi} = k_3 \begin{bmatrix} 0 & 0 \\ 0 & 0 \\ H_1^i & 0 \\ 0 & 0 \\ 0 & 0 \\ H_2^i & 0 \\ \dots & \dots \\ 0 & 0 \\ 0 & 0 \\ H_4^i & 0 \end{bmatrix} \tag{16}$$

$$\mathbf{C}_j = -\alpha(t) c_1 \begin{bmatrix} 0 & 0 & 0 & 0 & 0 & 0 & 0 & 0 & 0 & 0 & 0 & 0 \\ 0 & 0 & 0 & 0 & 0 & 0 & 0 & 0 & 0 & 0 & 0 & 0 \\ 0 & 0 & H_1^j H_1^j & 0 & 0 & H_1^j H_2^j & 0 & 0 & H_1^j H_3^j & 0 & 0 & H_1^j H_4^j \\ 0 & 0 & 0 & 0 & 0 & 0 & 0 & 0 & 0 & 0 & 0 & 0 \\ 0 & 0 & 0 & 0 & 0 & 0 & 0 & 0 & 0 & 0 & 0 & 0 \\ 0 & 0 & H_2^j H_1^j & 0 & 0 & H_2^j H_2^j & 0 & 0 & H_2^j H_3^j & 0 & 0 & H_2^j H_4^j \\ \dots & \dots & \dots & \dots & \dots & \dots & \dots & \dots & \dots & \dots & \dots & \dots \\ 0 & 0 & 0 & 0 & 0 & 0 & 0 & 0 & 0 & 0 & 0 & 0 \\ 0 & 0 & 0 & 0 & 0 & 0 & 0 & 0 & 0 & 0 & 0 & 0 \\ 0 & 0 & H_3^j H_1^j & 0 & 0 & H_3^j H_2^j & 0 & 0 & H_3^j H_3^j & 0 & 0 & H_3^j H_4^j \end{bmatrix}$$

$$\mathbf{K}_j = -k_1 \begin{bmatrix} 0 & 0 & 0 & 0 & 0 & 0 & 0 & 0 & 0 & 0 & 0 & 0 \\ 0 & 0 & 0 & 0 & 0 & 0 & 0 & 0 & 0 & 0 & 0 & 0 \\ 0 & 0 & H_1^j H_1^j & 0 & 0 & H_1^j H_2^j & 0 & 0 & H_1^j H_3^j & 0 & 0 & H_1^j H_4^j \\ 0 & 0 & 0 & 0 & 0 & 0 & 0 & 0 & 0 & 0 & 0 & 0 \\ 0 & 0 & 0 & 0 & 0 & 0 & 0 & 0 & 0 & 0 & 0 & 0 \\ 0 & 0 & H_2^j H_1^j & 0 & 0 & H_2^j H_2^j & 0 & 0 & H_2^j H_3^j & 0 & 0 & H_2^j H_4^j \\ \dots & \dots & \dots & \dots & \dots & \dots & \dots & \dots & \dots & \dots & \dots & \dots \\ 0 & 0 & 0 & 0 & 0 & 0 & 0 & 0 & 0 & 0 & 0 & 0 \\ 0 & 0 & 0 & 0 & 0 & 0 & 0 & 0 & 0 & 0 & 0 & 0 \\ 0 & 0 & H_3^j H_1^j & 0 & 0 & H_3^j H_2^j & 0 & 0 & H_3^j H_3^j & 0 & 0 & H_3^j H_4^j \end{bmatrix}$$

$$\mathbf{C}_{pj} = a(t)\begin{bmatrix} 0 & 0 \\ 0 & 0 \\ c_1 H_1^j & -c_2 H_1^j \\ 0 & 0 \\ 0 & 0 \\ c_1 H_2^j & -c_2 H_2^j \\ \dots & \dots \\ 0 & 0 \\ 0 & 0 \\ c_1 H_4^j & -c_2 H_4^j \end{bmatrix} \qquad \mathbf{K}_{pj} = k_1\begin{bmatrix} 0 & 0 \\ 0 & 0 \\ H_1^j & 0 \\ 0 & 0 \\ 0 & 0 \\ H_2^j & 0 \\ \dots & \dots \\ 0 & 0 \\ 0 & 0 \\ H_4^j & 0 \end{bmatrix}$$

with

$$k_1 = k_{leg}(1 - L_0 / L_l(t)),\ k_2 = k_{leg}(1 - L_0 / L_l(t))\left(\sum_{i=1}^{N} d_i / u - 1\right),$$

$$k_3 = k_{leg}(1 - L_0 / L_t(t))\ , k_4 = k_{leg}(1 - L_0 / L_t(t))\left(1 - \sum_{i=1}^{N-1} d_i / u\right) \tag{17}$$

$$c_1 = c_{leg}\sin^2\theta_l\ , c_2 = c_{leg}\sin\theta_l\cos\theta_l,\ c_3 = c_{leg}\sin^2\theta_t\ , c_4 = c_{leg}\sin\theta_t\cos\theta_t$$

As can be seen from Fig. 3, the pedestrian is acted upon by the contact forces $F_{s,t}$, $F_{d,t}$, $F_{s,l}$, $F_{d,l}$, G, F_I. Hence, the equations of equilibrium for the pedestrian body are

$$m_h \ddot{z} + F_{z,i} + F_{z,j} + m_h g = 0 \tag{18-a}$$

$$m_h \ddot{u} - F_{x,j} + F_{x,i} = 0 \tag{18-b}$$

Substituting Eqs. (13), (14) and (7) into Eq. (18) gives

$$\mathbf{M}_h \ddot{\mathbf{u}}_h + \mathbf{C}_h \dot{\mathbf{u}}_h + \mathbf{K}_h \mathbf{u}_h + \mathbf{C}'_{pi}\dot{\mathbf{u}}_i^e + \mathbf{C}'_{pj}\dot{\mathbf{u}}_j^e + \mathbf{K}'_{pi}\mathbf{u}_i^e + \mathbf{K}'_{pj}\mathbf{u}_j^e = \mathbf{F}_h(t) \tag{19}$$

where

$$\mathbf{M}_h = \begin{bmatrix} m_h & 0 \\ 0 & m_h \end{bmatrix} \qquad \mathbf{K}_h = \begin{bmatrix} k_1 + k_3 & 0 \\ 0 & k_4 - k_2 \end{bmatrix}$$

$$\mathbf{C}_h = \begin{bmatrix} \alpha(t)c_1 + (1-\alpha(t))c_3 & (1-\alpha(t))c_4 - \alpha(t)c_2 \\ (1-\alpha(t))c_4 - \alpha(t)c_2 & \alpha(t)(c_{leg} - c_1) + (1-\alpha(t))(c_{leg} - c_3) \end{bmatrix}$$

$$\mathbf{C}'_{pi} = -(1-a(t))\begin{bmatrix} 0 & 0 & c_3 H_1^i & 0 & 0 & c_3 H_2^i & \dots & 0 & 0 & c_3 H_4^i \\ 0 & 0 & c_4 H_1^i & 0 & 0 & c_4 H_2^i & \dots & 0 & 0 & c_4 H_4^i \end{bmatrix} \tag{20}$$

$$\mathbf{C}'_{pj} = a(t)\begin{bmatrix} 0 & 0 & -c_1 H_1^j & 0 & 0 & -c_1 H_2^j & \dots & 0 & 0 & -c_1 H_4^j \\ 0 & 0 & c_2 H_1^j & 0 & 0 & c_2 H_1^j & \dots & 0 & 0 & c_2 H_1^j \end{bmatrix}$$

$$\mathbf{K}'_{pi} = \begin{bmatrix} 0 & 0 & -k_3 H_1^i & 0 & 0 & -k_3 H_2^i & \dots & 0 & 0 & -k_3 H_4^i \\ 0 & 0 & 0 & 0 & 0 & 0 & \dots & 0 & 0 & 0 \end{bmatrix}$$

$$\mathbf{K}'_{pj} = \begin{bmatrix} 0 & 0 & -k_1 H_1^j & 0 & 0 & -k_1 H_2^j & \dots & 0 & 0 & -k_1 H_4^j \\ 0 & 0 & 0 & 0 & 0 & 0 & \dots & 0 & 0 & 0 \end{bmatrix}$$

$$\mathbf{F}_h(t) = \begin{Bmatrix} -m_h g & 0 \end{Bmatrix}^T$$

2.3. Equation of motion of the HSI system

For a multi-degree-of-freedom structural system, its equation of motion takes the form

$$\mathbf{M}^s \ddot{\mathbf{q}}(t) + \mathbf{C}^s \dot{\mathbf{q}}(t) + \mathbf{K}^s \mathbf{q}(t) = \mathbf{F}(t) \tag{21}$$

Where $\mathbf{M}^s$, $\mathbf{C}^s$ and $\mathbf{K}^s$ are the mass, damping and stiffness matrices of structure alone; $\ddot{\mathbf{q}}(t), \dot{\mathbf{q}}(t)$ and $\mathbf{q}(t)$ are the acceleration, velocity and displacement vectors of the structure, respectively, while $\mathbf{F}(t) = \begin{Bmatrix} 0 & \dots & \mathbf{f}_i & \dots & \mathbf{f}_j & \dots & 0 \end{Bmatrix}^T$ is the external force vector at any time *t*.
Substituting Eq. (15) into Eq. (21) gives

$$\mathbf{M}^s \ddot{\mathbf{q}}(t) + \begin{bmatrix} \dots & \dots & \dots & \dots & \dots \\ \dots & \mathbf{c}_i - \mathbf{C}_i & \dots & \dots & -\mathbf{C}_{pi} \\ \dots & \dots & \mathbf{c}_j - \mathbf{C}_j & \dots & -\mathbf{C}_{pj} \\ \dots & \dots & \dots & \dots & \dots \\ \dots & \dots & \dots & \dots & 0 \end{bmatrix} \begin{Bmatrix} \dots \\ \dot{\mathbf{u}}_i^e \\ \dot{\mathbf{u}}_j^e \\ \dots \\ \dot{\mathbf{u}}_h \end{Bmatrix} + \begin{bmatrix} \dots & \dots & \dots & \dots & \dots \\ \dots & \mathbf{k}_i - \mathbf{K}_i & \dots & \dots & -\mathbf{K}_{pi} \\ \dots & \dots & \mathbf{k}_j - \mathbf{K}_j & \dots & -\mathbf{K}_{pj} \\ \dots & \dots & \dots & \dots & \dots \\ \dots & \dots & \dots & \dots & 0 \end{bmatrix} \begin{Bmatrix} \dots \\ \mathbf{u}_i^e \\ \mathbf{u}_j^e \\ \dots \\ \mathbf{u}_h \end{Bmatrix} = \mathbf{0} \tag{22}$$

Where $[\mathbf{c}_i]_{12\times12}$, $[\mathbf{c}_j]_{12\times12}$, $[\mathbf{k}_i]_{12\times12}$, $[\mathbf{k}_j]_{12\times12}$ are the damping and stiffness matrices of the *i*th and *j*th element, respectively.
Combining Eqs. (19) and (22) gives the equations of motion for the multiple degree-of-freedom HSI system.

$$\tilde{\mathbf{M}}\ddot{\tilde{\mathbf{q}}}(t) + \tilde{\mathbf{C}}\dot{\tilde{\mathbf{q}}}(t) + \tilde{\mathbf{K}}\tilde{\mathbf{q}}(t) = \tilde{\mathbf{F}}(t) \tag{23}$$

where $\tilde{\mathbf{M}}, \tilde{\mathbf{C}}$ and $\tilde{\mathbf{K}}$ are the overall mass, damping and stiffness matrices, respectively. $\tilde{\mathbf{q}}(t), \dot{\tilde{\mathbf{q}}}(t)$ and $\ddot{\tilde{\mathbf{q}}}(t)$ are the displacement, velocity and acceleration vectors of the HSI system. $\tilde{\mathbf{F}}(t)$ is force vector of the HSI system. Matrices $\tilde{\mathbf{M}}$, $\tilde{\mathbf{C}}$, $\tilde{\mathbf{K}}$, vectors $\tilde{\mathbf{F}}(t)$ and $\tilde{\mathbf{q}}(t)$ are determined using the following expressions.

$$\tilde{\mathbf{M}} = \begin{bmatrix} \mathbf{M}^s & 0 \\ 0 & \mathbf{M}_h \end{bmatrix} \tag{24-a}$$

$$\tilde{\mathbf{C}} = \begin{bmatrix} \dots & \dots & \dots & \dots & \dots \\ \dots & \mathbf{c}_i - \mathbf{C}_i & \dots & \dots & -\mathbf{C}_{pi} \\ \dots & \dots & \mathbf{c}_j - \mathbf{C}_j & \dots & -\mathbf{C}_{pj} \\ \dots & \dots & \dots & \dots & \dots \\ \dots & \mathbf{C}'_{pi} & \mathbf{C}'_{pj} & \dots & \mathbf{C}_h \end{bmatrix} \tag{24-b}$$

$$\tilde{\mathbf{K}} = \begin{bmatrix} ... & ... & ... & ... & ... \\ ... & \mathbf{k}_i - \mathbf{K}_i & ... & ... & -\mathbf{K}_{pi} \\ ... & ... & \mathbf{k}_j - \mathbf{K}_j & ... & -\mathbf{K}_{pj} \\ ... & ... & ... & ... & ... \\ ... & \mathbf{K}'_{pi} & \mathbf{K}'_{pj} & ... & \mathbf{K}_h \end{bmatrix} \tag{24-c}$$

$$\tilde{\mathbf{F}}(t) = \begin{Bmatrix} 0 & ... & -m_h g & 0 \end{Bmatrix}^T \tag{24-d}$$

$$\tilde{\mathbf{q}}(t) = \begin{Bmatrix} q_1 & q_2 & ... & z & u \end{Bmatrix}^T \tag{24-e}$$

It is noted from Eqs. (16) and (20) that matrices $\mathbf{C}_i$, $\mathbf{C}_j$, $\mathbf{C}_{pi}$, $\mathbf{C}_{pj}$, $\mathbf{C}_{pi}^{'}$, $\mathbf{C}_{pj}^{'}$, $\mathbf{K}_i$, $\mathbf{K}_j$, $\mathbf{K}_{pi}$, $\mathbf{K}_{pj}$, $\mathbf{K}_{pi}^{'}$ and $\mathbf{K}_{pj}^{'}$ are time-varying depending on the dynamic responses of both the plate and human. Hence, the damping and stiffness matrices of the HSI system are time-dependent, while the mass matrix is constant throughout the walking process.
The dimensions of overall mass, damping and stiffness matrices of the HSI system are equal to the sum of the dimensions of the structure and the pedestrian, i.e. $3(n+1)(m+1)+2$.

2.4. Feedback mechanism

A damped compliant bipedal walking model is able to reproduce a one-step gait cycle that consists of the single and double support phases. This model requires an energy input to maintain the steady walking gait because energy has been dissipated with the system damping in the walking process. This energy consumption is distributed throughout the gait cycle (Whittington and Thelen, 2009). One possible candidate, among many ways to provide this additional energy, is to apply a control force to the system in a feedback or feed-forward manner (Kim and Park, 2011). The control force is applied by the pedestrian to maintain the total energy of the human body during walking.
A horizontal control force is applied in this study to maintain equilibrium of energy in the system. The control force can be calculated from the following equation (Qin et al, 2013)

$$F_{ctr}(t) = \frac{E_0 - E(t) + m_h \cdot g \cdot \omega(t)}{\Delta u(t)} \tag{25}$$

where $F_{ctr}(t)$, E_0 and $E(t)$ are the horizontal control force, initial energy input, energy of the human body respectively; $\omega(t)$ and $\Delta u(t)$ are the vertical deflection of the floor and horizontal displacement increment of the CoM at time '*t*', respectively.
The total energy of the human body, $E(t)$, including the potential energy and the kinetic energy is given by.

$$E(t)=\frac{1}{2}m_h v_z^2+\frac{1}{2}m_h v_x^2+\frac{1}{2}k_{leg}(\Delta L_l)^2+\frac{1}{2}k_{leg}(\Delta L_t)^2+m_h gz \tag{26}$$

where v_z and v_x are the vertical and horizontal velocity of CoM.
With the above considerations, the force vector in Eq. (22) is then revised as

$$\tilde{\mathbf{F}}(t)=\left[0,0,.....,-m_h g,F_{ctr}(t)\right]_{3\times(n+1)(m+1)+2}^{T} \tag{27}$$

3. Computational procedures

The solution procedures are as follows:
(1) Input the geometric and physical parameters of the floor and pedestrian.
(2) Construct the mass matrix $\mathbf{M}^s$,stiffness matrix $\mathbf{K}^s$ and damping matrix $\mathbf{C}^s$ of the floor alone.
(3) Specify the initial conditions of the floor and the pedestrian with the following data: (a) initial displacement and velocity of the COM at time *t=0*; (b) the position for the first leg to touch down; (c) time increment Δt ; (d) initial step number *st*=1;
(4) Construct the overall mass, stiffness and damping matrices of the HSI system at time *t=0*. Then compute the initial acceleration of the HSI system with

$$\ddot{\tilde{\mathbf{q}}}_0=\tilde{\mathbf{M}}^{-1}\left(\tilde{\mathbf{F}}_0-\tilde{\mathbf{C}}\dot{\tilde{\mathbf{q}}}_0-\tilde{\mathbf{K}}\tilde{\mathbf{q}}_0\right)$$

(5) Calculating the following for each time step,
5.1 Determine the plate elements i and j on which the pedestrian locates with the followings

i= integer part of $(\bar{y}_{cj}/b)\times m$ +integer part of $(\sum_{k=1}^{N-1}d_k/a)$ +1, (trailing leg)

j= integer part of $(\bar{y}_{cj}/b)\times m$ +integer part of $(\sum_{k=1}^{N}d_k/a)$ +1, (leading leg)

where a and b are the width and length of the plate element as shown in Fig. 2.
5.2 Determine the time dependent position of the pedestrian x_{ci}, x_{cj} (local coordinates) on the *i*th and *j*th element with the followings:

$$x_{ci}=\sum_{k=1}^{N-1}d_k-(i-1)a\,,\qquad x_{cj}=\sum_{k=1}^{N}d_k-(j-1)a$$

5.3 Compute the shape functions from Eq. (10).
5.4 Determine the displacement and velocity at the foot contact point with the slab from Eqs. (13) and (14).
5.5 Compute the length of two legs from Eq. (2) and determine the coefficients from Eq. (15).

5.6 Determine the mass, damping and stiffness matrices of the moving element from Eqs. (16) and (20).
5.7 Solve the equation of motion Eq. (23) with the Newton-Raphson's method (Chopra, 1995) to determine the dynamic responses of the HSI system.
5.8 Determine if a new step cycle is needed from
(a) Compute the displacement and velocity at the foot contact point with the slab at the end of the time increment from Eqs. (13) and (14). Then determine the length of trailing leg from Eq. (2).
(b) If the length of the trailing leg is larger than the rest length of leg, the single support phase starts and the distance from the CoM to the newly assumed foot contact point for the next step cycle is computed.
(c) If the rest length of leg lies between the distances from the CoM to the foot contact point at the last time step, $L_{I-1} = \sqrt{\left(z_{I-1} - y\big|_{I-1}\right)^2 + (L_0 \sin\theta_0)^2}$, and the assumed contact point at the current time step, $L_I = \sqrt{\left(z_I - y\big|_I\right)^2 + (L_0 \sin\theta_0)^2}$, set step number *st=st+1* and the double support phase of the new step cycle begins.
5.9 Compute the control force from Eq. (25) and then revise the overall force vector from Eq. (27).
5.10 Determine the acceleration of the HSI system at the end of time increment using the follows:

$$\ddot{\tilde{\mathbf{q}}}(t+\Delta t) = \tilde{\mathbf{M}}^{-1}\left(\tilde{\mathbf{F}}_i(t+\Delta t) - \tilde{\mathbf{C}}\dot{\tilde{\mathbf{q}}}(t+\Delta t) - \tilde{\mathbf{K}}\tilde{\mathbf{q}}(t+\Delta t)\right)$$

5.11 Repeat Steps 5.1 to 5.10 to obtain the dynamic responses of the HSI system for next time step until the pedestrian moves outside the plate.

4. Ground reaction force

The characteristic properties of the human body are:- the leg stiffness k_{leg}=21 kN/m, damping ratio of human body ξ=8%, human mass m_h=80 kg, angle of attack θ_0=68° and initial energy input E_0=825 J. The last one is determined from trial and error to have a steady walking gait for a limited number of footstep cycles without faltering. The angle of attack θ_0 is assumed constant in walking.
The ground reaction force (GRF) time histories generated by using the bipedal walking model are plotted in Fig. 4. It clearly shows that a time-dependent damper is necessary to ensure that the ground reaction force is zero when the leg touches down at the start of each step cycle. Otherwise, the damping force generated by the pedestrian will not be zero when the leg touches down at the start of each step cycle because the axial spring velocity is not zero. As a result, the GRF is also not equal to zero. A typical continuous ground reaction force time history is shown in Fig 5. The walking pace is approximately 2.02 Hz and the average walking speed is around 1.25 m/s. If the horizontal control force is not applied, the pedestrian footstep would stumble after a limit number of step cycles.

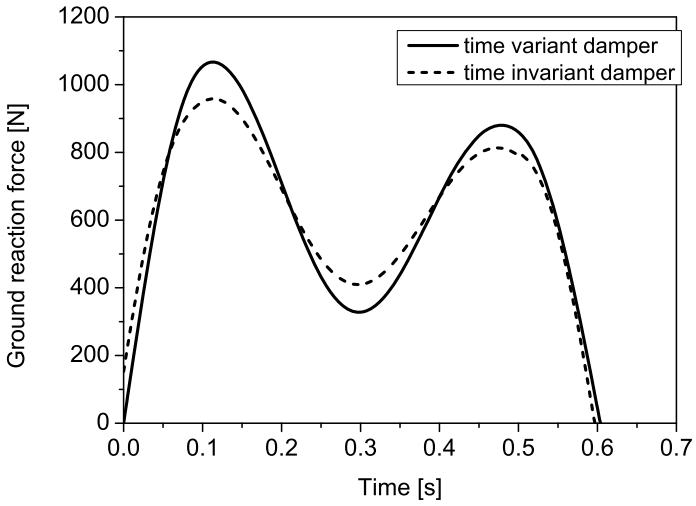

Fig. 4 Ground reaction force by bipedal walking model of a 80kg pedestrian

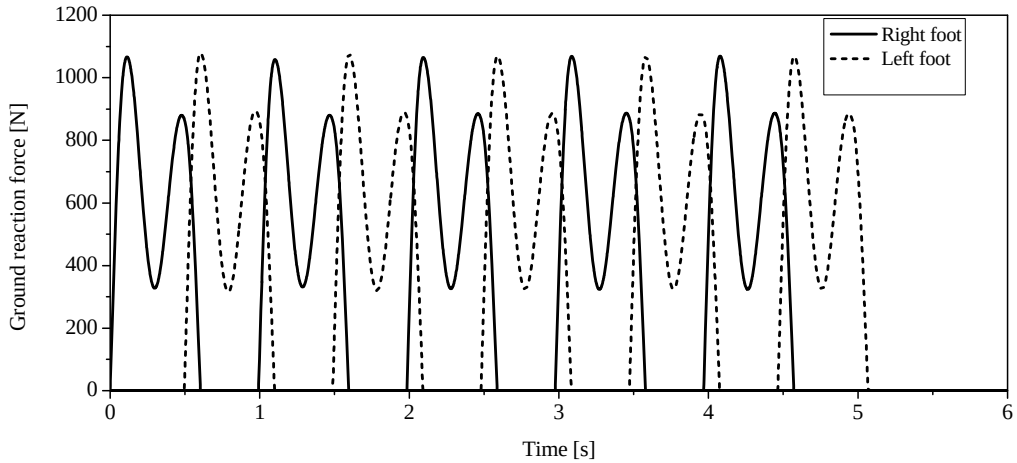

Fig. 5 Continuous ground reaction force of a 80kg pedestrian pacing at 2.02 Hz

5. SIMULATION STUDIES

To illustrate the features of the proposed interaction model, two examples of human-structure interaction are analyzed. The results from using bipedal walking model are compared with those from using time domain force model, which is the most common existing model to analyze for the dynamic behavior of floors.

All the results presented in this section are based on the acceleration of gravity g=9.8m/s^2 and the time interval Δt =0.001 second. Besides, the overall damping matrix $[\tilde{C}]$ is obtained based on the damping ratios $\xi_1 = \xi_2$ = 0.005 and the associated natural frequencies ω_1 and ω_2.

5.1. Example 1 - Stiff floors

Considering a simply supported floor slab subjected to pedestrian motion. The floor slab is 1.0 m wide and 0.35 m deep and with a 6.0 m simply supported span. The material properties of the slab are mass density ρ=2400 kg/m^3, Young's modulus E = 3.0×10^{10} N/m^2 and Poisson ratio 0.2. The information of the human body is exactly the same as that in Section 4.

The floor is modeled with 20×5 finite plate elements. The fundamental frequency of the slab alone is 15.56 Hz. Generally this floor slab is typically stiff because its fundamental frequency is above 10 Hz. Fig. 6 give the dynamic responses at midspan of the slab. The dash-dot line denotes the dynamic responses of the plate under the force time histories as shown in Fig. 5. It is clear that the response of the stiff floor is transient. Each peak response is associated with a heel impact followed by vibration with a rate of decay associated with the structural damping. The small differences between the two sets of curves from the bipedal walking model and the force time history model indicate that the proposed formulation is appropriate for the human-structure interaction studies.

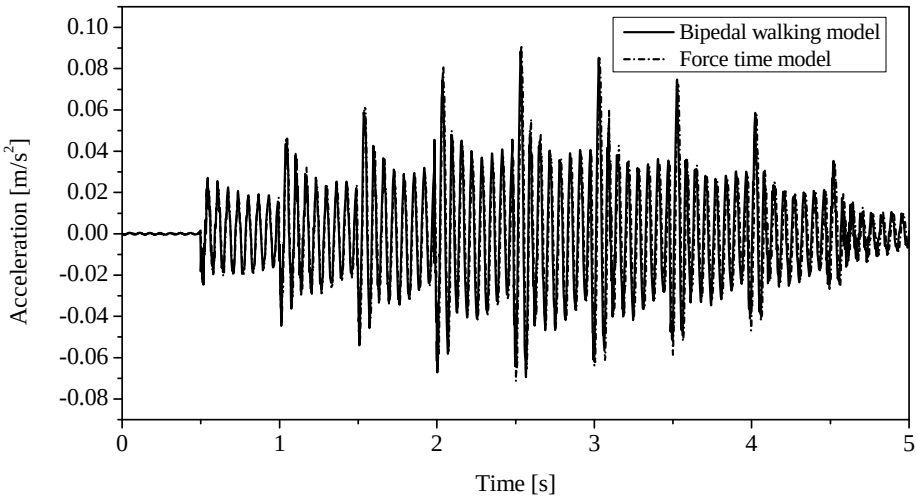

Fig. 6 Acceleration at the midspan of a stiff floor

The dynamic behavior of the pedestrian can also be obtained from the equation of motion of the system in Eq. (23). Fig. 7 and 8 show the vertical displacement and acceleration of CoM in the walking process. The dynamic responses of human body are noted steady. The ground reaction forces generated by human across the floor (not shown) are very similar to those in Fig. 5 because both cases have a regular pattern of footstep forces.

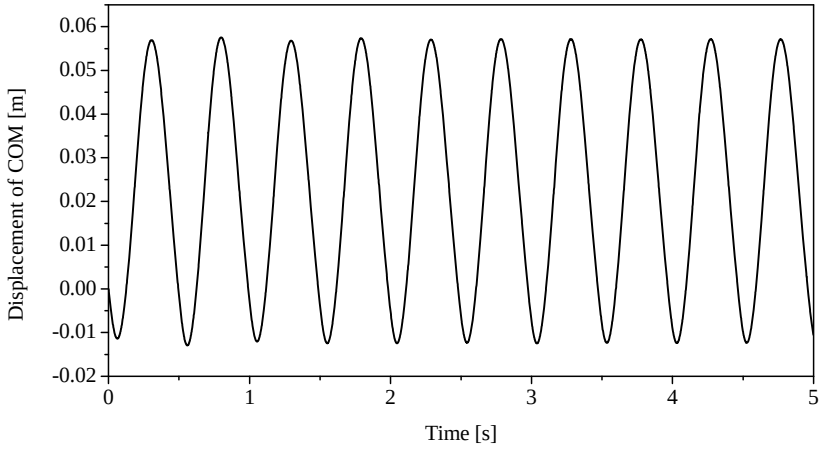

Fig. 7 Displacement of CoM in walking process

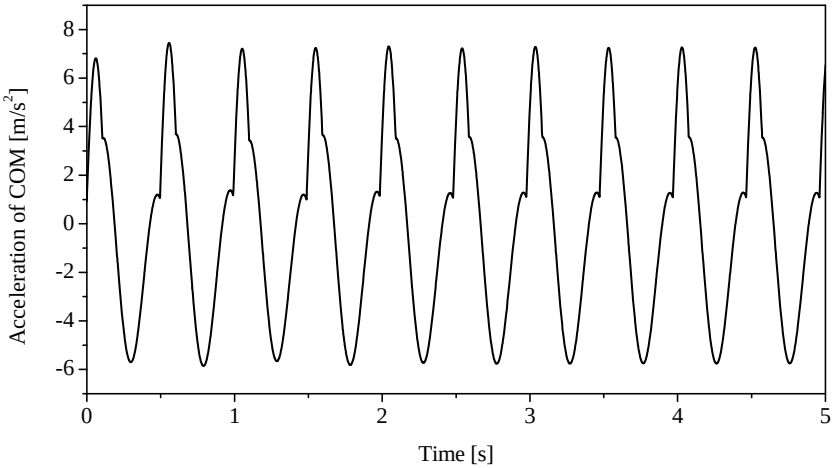

Fig. 8 Acceleration of CoM in walking process

The above results show that the dynamic interaction of human-structure system is small when the natural frequency of floor is high.

5.2 Example 2 - Flexible floors

Considering a simply supported floor with 1.0 m wide and 0.15 m deep slab with 8.0 m span subjected to a pedestrian motion. The material properties of the floor and information of the human body are the same as those in Section 5.1.
The floor is also modeled with 20×5 finite plate elements. The fundamental frequency of the floor slab alone is 3.76 Hz. The acceleration response at the center of floor is plotted in Fig. 9. The more distinctive differences between the two sets of curves reveal that the dynamic interaction of the human-structure system is significant. This is due to the fact that the compression of the legs will be larger with greater vibration of the floor. Therefore, the elastic potential energy stored in the compliant leg at the end of the single support phase of each step cycle, which serves as the propulsion energy during

push-off, becomes larger when the pedestrian moves towards midspan of the floor. As a result, the dynamic behavior of the human body is not the same for each step cycle of walking as shown in Fig. 10. Moreover, the interaction footstep forces generated by the pedestrian gradually increases with the pedestrian moving towards midspan of the plate as shown in Fig. 11.

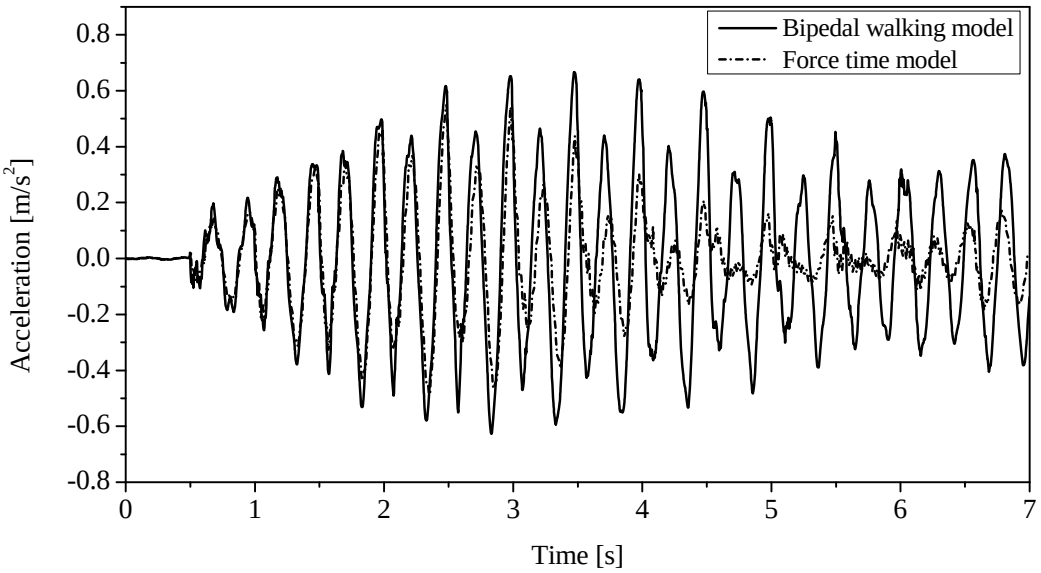

Fig.9 Acceleration at the midspan of low frequency floor

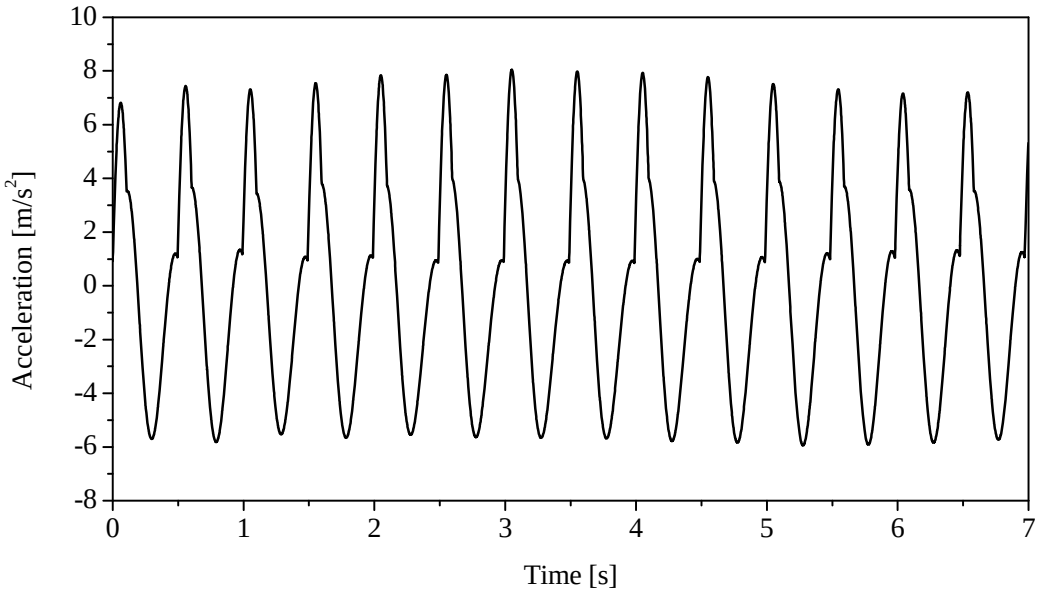

Fig.10 Acceleration of CoM in walking process

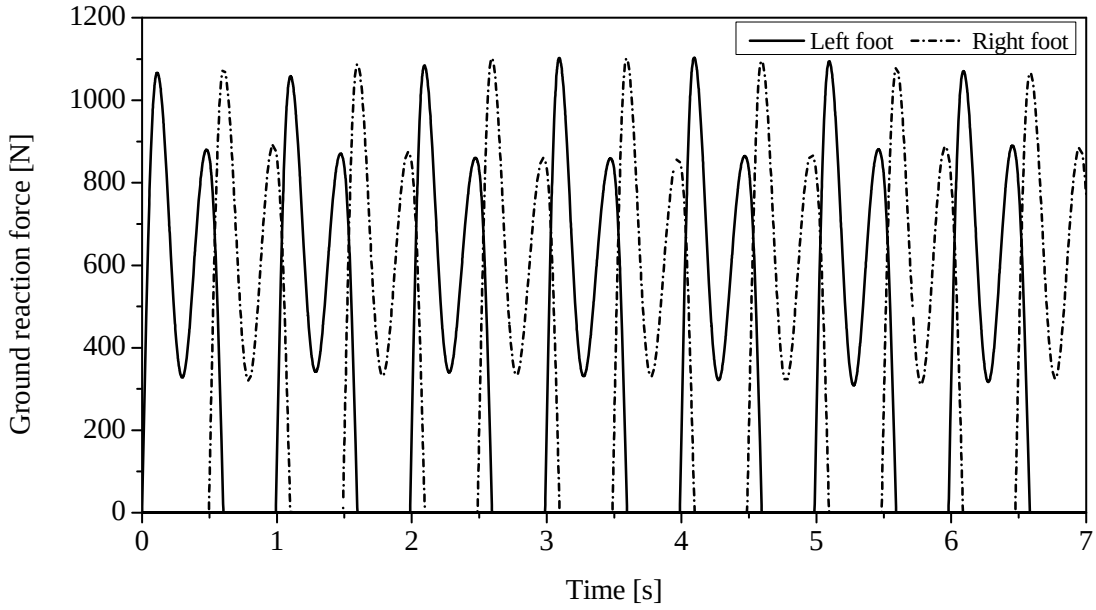

Fig. 11 Ground reaction force generated in walking process

These results show that the proposed formulation on the modeling of the pedestrian-floor interaction could describe properly the human-structure interaction. The time force history model is not suitable for the dynamic analysis of slender structures, such as a long span floor, as it does not consider the effects from human-structure interaction and the adjustment made by the pedestrian to maintain a steady gait.

6. DISCUSSION

The bipedal walking model with damped compliant leg can reproduce a one-step gait cycle that consists of the single and double support phases. It can be adopted to describe the human-structure interaction in this study. The current bipedal walking model is improved with the assumption of time dependent damping and a feedback control force applied by pedestrian to maintain the steady gait. The leg axial velocity is not zero when the leg touches down at the start of the gait cycle. This implies that the leading leg damping must be zero at the start of the cycle. A control force in a feedback manner is applied by the pedestrian to compensate for energy dissipated with the system damping in walking and to regulate the walking behavior of the pedestrian. As mentioned previously, a control force is only one possible candidate, among many ways, to provide the additional energy. Many tests have shown that the leg stiffness can be adjusted to enable similar or uniform gait cycle in the process (Ferris and Farley, 1997; Farley, et al, 1998; Grimmer, et al, 2006; Mueller, et al, 2010). It should be noted that real humans might not adjust the leg properties in this way. However, how the leg

stiffness is adjusted is still not clear and not reported. The dynamic behavior of CoM is noted to be uniform in each step cycle with the horizontal control force applied by pedestrian. Nevertheless, the model in its current form can show how humans might interact with the bridge. The modeling procedure has more general application as when the gait conditions are varied dynamically, the leg parameters are also varied actively. Both previously published mechanisms and the present actuator mechanism represent the potential complexities of human walking, and they have been successful in the sense to illustrate that stable walking under lateral and vertical perturbation is possible using a simple control law. Such simple models may break down in regimes of high frequency or high amplitude perturbation whereby an extension of the present model could possibly be viable for further study.

7.CONCLUSION

The proposed interaction model provides a means to understand how the structural vibration can influence the walking behavior of a pedestrian and how a pedestrian can respond to the vibration level of structure to maintain a steady gait, which in turn affects the dynamic responses of the structure. Simulation results show that the dynamic interaction will increase with a larger vibration level of structure. More external energy must be input to maintain a steady walking and uniform dynamic behavior of the pedestrian in the process.

ACKNOWLEDGEMENTS

This research was supported by the Research Program funded by the National Natural Science Foundation of China (No. 50725826 & 50938008) and the Niche Area Project Funding of the Hong Kong Polytechnic University Project (No.1-BB6F).

REFERENCES

Bocian, M., Macdonald, J. H. G. and Burn, J. F. (2012), “Biomechanically inspired modeling of pedestrian-induced forces in laterally oscillating structures.” Journal of Sound and Vibration, 331, 3914-3929.

Chopra, A. K. (1995), Dynamics of Structures: Theory and Applications to Earthquake Engineering. Englewood Cliffs, NJ, USA: Prentice Hall.

Farley, C. T., Houdijk, H. H., Van Strien, C. and Louie, M. (1998), “Mechanism of leg stiffness adjustment for hopping on surfaces of different stiffnesses.” Journal of Applied Physiology, 85, 1044-1055.

Ferris, D. P., and Farley, C. T. (1997), “Interaction of leg stiffness and surfaces stiffness during human hopping.” Journal of Applied Physiology, 82, 15-22.

Geyer, H., Seyfarth, A., and Blickhan, R. (2006), “Compliant leg behavior explains basic dynamics of walking and running.” Proceedings of the Royal Society B: Biological Sciences, 273, 2861–2867.

Grimmer, S., Ernst, M., Guenther, M., and Blickhan, R. (2008), “Running on uneven ground: leg adjustment to vertical steps and self-stability.” Journal of Experimental Biology, 211 (18), 2989-3000.

İsmail, Esen. (2011), “Dynamic response of a beam due to an accelerating moving mass using moving finite element approximation.” Mathematical and Computational Applications, Vol. 16, No. 1, 171-182.

Kim, S., and Park, S. (2011), “Leg stiffness increases with speed to modulate gait frequency and propulsion energy.” Journal of Biomechanics, 44, 1253–1258.

Kown, Y.W., Bang, H. (1997), The finite element method using Matlab. CRC process, New York,

Mueller, R., Grimmer, S. and Blickhanm R. (2010), “Running on uneven ground: Leg adjustments by muscle pre-activation control.” Human Movement Science, 29 (2), 299-310.

Macdonald, J.H.G. (2008), “ Lateral excitation of bridges by balancing pedestrians.” Proceedings of the royal society A, 465, 1055-1073.

Moriato, T., Vitaliani, R. and Saetta, A. (2011), “Numerical analysis of a synchronization phenomenon: Pedestrian-structure interaction.” Computer and Structures, 89, 1649-1663.

Qin, J.W., Law, S.S., Yang, Q.S. and Yang, N.(2013), “Pedestrian-Bridge Dynamic Interaction Including Human Participation.” Journal of Sound and Vibration, 332, 1107-1124.

Whittington, B. R. and Thelen, D. G. (2009), “A simple mass-spring model with roller feet can induce the ground reactions observed in human walking.” Journal of Biomechanical Engineering, 131, 011013-1–011013-8.

Wu, J.J. (2008), “Transverse and longitudinal vibrations of a frame structure due to a moving trolley and the hoisted object using moving finite element.” International Journal of Mechanical Sciences, 50, 613–625.

Yang, Y. B., Chang, C. H. and Yau, J. D. (1999), “An element for analyzing vehicle bridge system considering vehicle’s pitching effect.” Inernational Journal for numerical methods in engineering, 46, 1031-1047.

Yang, Y. B., and Wu, Y. S. (2001), “A versatile element for analyzing vehicle–bridge interaction response.” Engineering Structures, 23, 452–469